

Switching in the presence of colored noise: The decay of an unstable state

Mark James*

Department of Physics, University of Lancaster, Lancaster LA1 4YB, United Kingdom

Frank Moss

Department of Physics, University of Missouri at St. Louis, St. Louis, Missouri 63121

Peter Hänggi

Institute of Mathematics, University of Augsburg, D-8900 Augsburg, Federal Republic of Germany

Christian Van den Broeck

Limburgs Universitair Centrum, B-3610 Diepenbeek, Belgium

(Received 14 March 1988; revised manuscript received 29 June 1988)

Switching events are studied by means of a parametrically operated, fast transition from a monostable to a bistable potential in the continuous presence of colored noise. The problem is thus the decay of an unstable state with random initial conditions. We calculate, using contemporary colored-noise theory, and measure by analog simulation, the relaxation time to cross a reference boundary, and we contrast this with the strictly defined mean first passage time.

I. INTRODUCTION

In this paper we study a switching process under the influence of noise which is common to a class of parametrically activated bistable systems. The system exhibits a single, or monomodal, state x_0 while inactive, but develops a bimodal potential upon receipt of a parametric switching signal. The bimodal potential is developed in a time which is short compared to the characteristic dynamical response time of the system. The initial state x_0 thus becomes an unstable state at the instant when the switching signal is received. This state is, however, perturbed by noise which drives the decay. After a relaxation time $\langle T \rangle$, which we analyze and measure herein, the system settles into one of the bistable states.

Such generic switching processes were first proposed by Landauer¹ as possible zero- or low-energy switches. They have been used for quite some time as examples in discussions on the minimum energy dissipation necessary for measurement and for information transmission and computation.² In view of this interest and of the fundamental importance of the switching process itself, it is relevant to study the dynamics of switching in the presence of noise, which is inescapable in macroscopic systems.

The first theory and measurements on such noisy switching events induced by linearly swept parameters and their remarkable noise-averaging properties were carried out by Kondepudi *et al.*³ Noisy switching events in lasers have been studied experimentally by Zhu *et al.*^{4(a)} and analytically by Broggi *et al.*^{4(b)} and later simulated with analog circuits.⁵ However, all of these studies were of switching events induced by variations of the parameters on time scales comparable to the characteristic dynamical response time of the system. By contrast in the present study the switch parameter is operated by a step function at time $t=0$, thus preparing an initial state

which later decays into the induced bistable states.

The problem of the decay of an unstable state in the presence of *white* noise has been well studied by a variety of techniques.^{6,7} Among the more familiar and useful methods for describing the onset of macroscopic order are the time evolution of the variance $\langle x^2 \rangle(t)$, the mean first passage time (MFPT), and the onset of bimodality in the probability density. The MFPT in recent years has become a widely used tool for analyzing such stochastic processes.⁸

Non-numerical colored noise theories are, however, necessarily approximate. This arises because of the extra variable necessary to describe noise with nonzero correlation time. The Langevin equation and its analogous Fokker-Planck (FP) equation are, consequently, at least two dimensional. Since the latter equation can be solved exactly only in one dimension,⁹ recent years have witnessed a veritable explosion of approximative schemes,¹⁰⁻¹⁷ all of which seek to reduce the FP equation to an "equivalent" one-dimensional form, and an increasingly vigorous debate regarding their accuracy and applicability.^{14,17-19} With the exception of Refs. 12 and 14 all of these are adaptations of, or improvements on, an approximation originally put forth by Stratonovich^{20,21} based on expansions valid for small correlation times. How accurate they are for a given correlation time depends on the application and often the noise intensity as well. Here we present measurements for τ as large as $\tau=5$ for which both one- and two-dimensional stationary probability densities have been studied.^{9,12,22}

In this work the nonsmall noise color introduces difficulties at two levels. In order to calculate the stationary mean-square fluctuation intensity in the initial state, we will use a simple linearization which is expected to be accurate for small noise intensities. More detailed theories such as those cited above could be used instead, but the linear theory is sufficiently accurate for the

initial-state calculations. We then analyze the transient relaxation toward the stable state using colored-noise modified Suzuki scaling⁶ following a recent theory.²³ These results are then compared to measurements made on an analog simulator of an example switch.

We find that the relaxation time is a decreasing logarithmic function of the noise intensity, results that, for white noise, were anticipated much earlier.^{6,24-31} Increasing the noise correlation time increases the relaxation time but does not have a large effect.

This paper is organized as follows. In Sec. II the theory is developed following Refs. 12 and 23. In Sec. III the simulator, its operation, and the measurement techniques are described. The results are presented in Sec. IV and compared to the calculations. Conclusions and a discussion are presented in Sec. V.

II. THEORY

First we consider the stationary dynamics in a single-well potential, i.e., before the control-parameter-induced switching event. The potential is given by

$$U(x) = \frac{1}{2}[x^2 - A \ln(1+x^2)], \quad (1a)$$

and the forcing is

$$f(x) = x[-1 + A(t)/(1+x^2)], \quad (1b)$$

where $A(t)$ is the control parameter. As shown in Fig. 1, the potential is monostable for $A < 1$ and bistable for $A > 1$. Moreover, the width of the monostable potential depends upon $|A|$. Our model is determined by the Langevin equation

$$\dot{x} = f(x) + \xi(t), \quad (2a)$$

where $\xi(t)$ is an exponentially correlated, Gaussian noise source with zero mean:

$$\langle \xi(t)\xi(s) \rangle = (D/\tau)\exp(-|t-s|/\tau), \quad (2b)$$

where D is the noise intensity and τ is the noise correlation time. The system is prepared in the monostable initial state by setting $A(t) = A_0 < 1$, for which the deterministic solution $x_0 = 0$, is globally stable. After having been prepared in this initial state for a time sufficiently

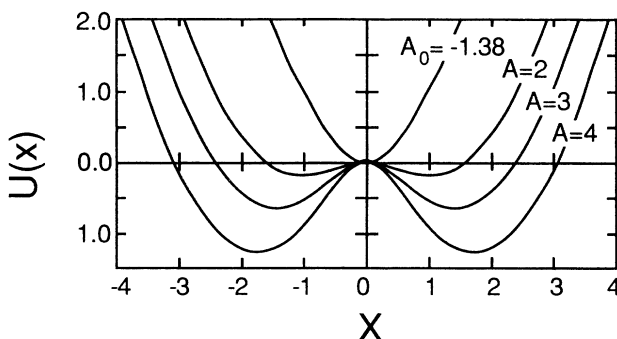


FIG. 1. The potential, showing a monostable initial state for $A_0 = -1.38$ and the switched bistable states at the values of A indicated.

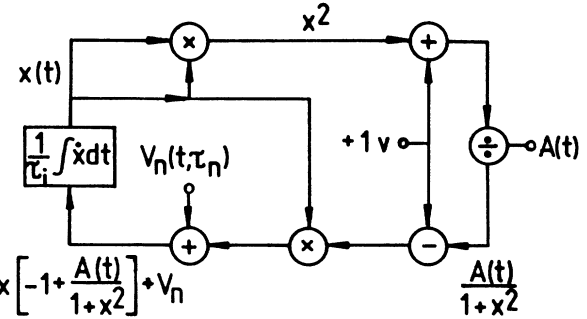


FIG. 2. The circuit diagram of the electronic simulator. The multipliers and the divider are standard chips available from Analog Devices, Norwood, Mass.

long to establish stationary statistical conditions, the system is switched at $t=0$ so that $A(t) = A > 1$ for all $t > 0$. The control parameter is thus a step function.

We first consider the initial state for which stationary conditions are assumed. In order to proceed it is necessary to obtain the stationary probability density. In fact, we will only need the second moment $\langle x^2 \rangle_{st} = \langle x_0^2(\tau) \rangle$ of the stationary initial distribution. Since both the experiment and the theory to be used later are restricted to small values of D , linearized theory will be sufficient for calculating $\langle x_0^2(\tau) \rangle$. We begin with the following FP equation, valid for small D :

$$\begin{aligned} \frac{\partial P(x, \xi, t)}{\partial t} = & \frac{\partial}{\partial x} \{ [(|A_0| + 1)x - \xi] P(x, \xi, t) \} \\ & + \frac{\partial}{\partial \xi} \left\{ \frac{\xi}{\tau} P(x, \xi, t) \right\} \\ & + \frac{D}{\tau^2} \frac{\partial^2}{\partial \xi^2} P(x, \xi, t). \end{aligned} \quad (3)$$

In the steady state, the equations for the moments read

$$(|A_0| + 1)\langle x_0^2(\tau) \rangle - \langle x\xi \rangle = 0, \quad (4)$$

$$(|A_0| + 1 + \tau^{-1})\langle x\xi \rangle - \langle \xi^2 \rangle = 0, \quad (5)$$

$$-\langle \xi^2 \rangle + \frac{D}{\tau} = 0, \quad (6)$$

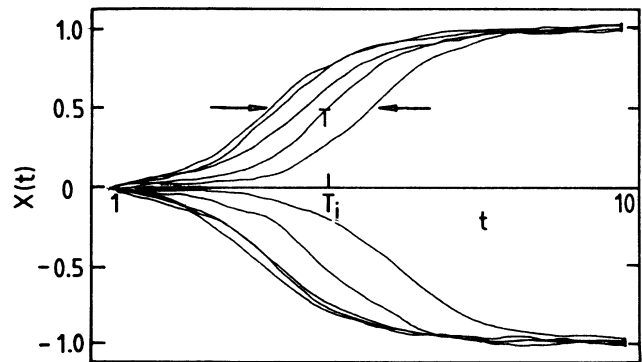


FIG. 3. Example trajectories measured for $A_0 = -1.38$ and $A = 2$ for $D = 0.1$ and $\tau = 1.0$. The bistable potential is switched at $t = 0$. The vertical scale is in volts with the potential minima at ± 1.0 V. The horizontal scale is in ms.

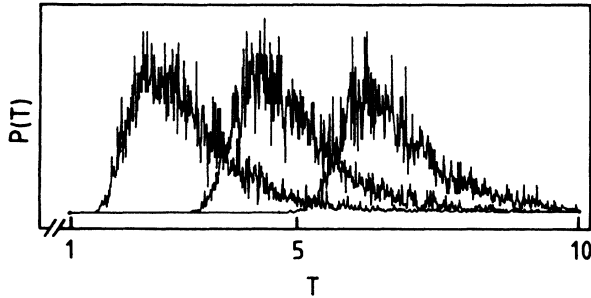


FIG. 4. Examples of the probability density of the relaxation time from which the $\langle T \rangle$ were obtained for $\tau=1.0$, $A=2.0$, $A_0=-1.38$, and, reading from left to right, $D_1=11.7 \times 10^{-3} \text{ V}^2$, $\langle T \rangle=2.4 \text{ ms}$; $D_2=0.20 \times 10^{-3} \text{ V}^2$, $\langle T \rangle=4.4 \text{ ms}$; and $D_3=2.56 \times 10^{-6} \text{ V}^2$, $\langle T \rangle=6.6$. The horizontal scale is in ms.

from which we conclude that

$$\langle x_0^2(\tau) \rangle = D \{ (1 + |A_0|) [1 + \tau(1 + |A_0|)]^{-1} + O(D^2) \}. \quad (7)$$

This describes the stationary dynamics before the switching event takes place.

For $t=0^+$, the system is switched to a bistable state as shown in Fig. 1 for $A > 0$, and the state at $x=0$ is rendered locally unstable. Since the switching event takes place in a time very short compared to all other time scales in the problem, the decay is driven by the noise dynamics described by Eqs. (6) and (7) toward the two locally stable states $x_s = \pm \sqrt{A-1}$ created at $t=0$.

The simulation, described in Sec. III, measures the residence time T , for a random walker $x(t)$ necessary to cross a reference value $x_R = x_s/2$ for the first time after the switch function is activated at $t=0$. The mean of this quantity $\langle T \rangle$ is a measure of the time scale on which the system assumes macroscopic order and is closely related to (but not identical with) the MFPT on the same interval. The residence time is like a weighted MFPT wherein the distribution of initial conditions is a Gaussian whose second moment is given by Eq. (7). By contrast, our switch is more physically realistic in supposing that the

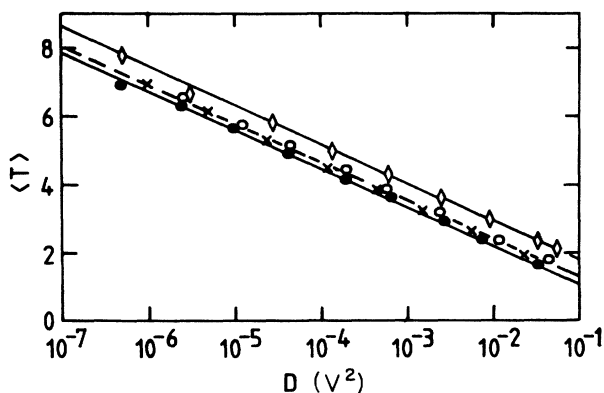


FIG. 5. $\langle T \rangle$ in ms vs D in V^2 for $A_0=-1.38$ and $A=2.0$. The values of τ are 0.1, 0.5, 1.0, and 4.9. The solid lines are fits to the data and the dashed line is a predicted result for $\tau=0.5$.

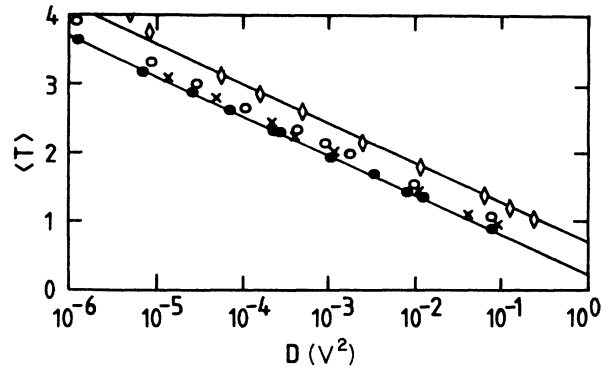


FIG. 6. $\langle T \rangle$ in ms vs D in V^2 for $A_0=-1.38$ and $A=3.0$. The values of τ are 0.1, 0.5, 1.0, and 4.9. The solid lines are fits to the data.

noise is continuously present, as it is in all real switches. In fact it is possible that the instant the unstable state is born, the trajectory $x_0(t=0)$ could already exceed the reference boundary x_R . For small D , however, in the range where both the theory and the simulation are accurate, such events are extremely rare.

The time for decay from an unstable state has been studied by many authors.^{6,26-31} As shown first by Kubo *et al.*,²⁶ the relaxation time exhibits a logarithmic dependence on the noise intensity. Very recently, Suzuki's scaling theory^{6,31} has been generalized to include colored noise,²³ with the result

$$\langle T \rangle = -(1/2\alpha) \ln(C \{ \langle x_0^2 \rangle + D[\alpha(1+\alpha\tau)]^{-1} \}), \quad (8)$$

where $\alpha \equiv f'(x=0^+) = A-1$, and where C is a constant that depends only on the parameters of the deterministic nonlinear flow $f(x)$, i.e., on A_0 and A , but not on D or τ . The theoretical value of C depends also on the detailed definition of the residence time, for example, as the time for the second moment $\langle x^2 \rangle(t)$ to relax to some reference value x_R , or the time required for $P(x, t)$ to become bimodal, or the strictly defined MFPT, etc. But certainly C is of order unity so that $\ln C$ is of order zero.

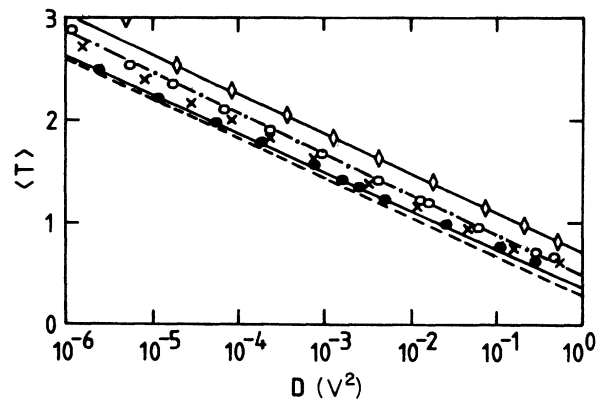


FIG. 7. $\langle T \rangle$ in ms vs D in V^2 for $A_0=-2.40$ and $A=4.0$. The values of τ are 0.1, 0.5, 1.0, and 5.0. The solid lines are fits to the data. The dot-dashed and dashed lines are theoretical predictions for $\tau=1.0$ and 0.1, respectively.

TABLE I. Calculated and measured parameters for $A_0 = -1.38$, $A = 2$, and $B_0 = -0.03$.

τ	m^{theor}	m^{expt}	$b^{\text{theor}}(\tau)$	$b^{\text{theor}}(\tau) + B_0$	b^{expt}
4.9	1.15	1.11	0.80	0.77	0.77
1.0	1.15	1.14	0.23	0.20	0.20
0.5	1.15	1.13	0.08	0.05	0.10
0.1	1.15	1.12	-0.11	-0.14	0.02

In our experiment, the noise color enters Eq. (8) in two places: First, there is a colored-noise effect on the initial state $P_0(x, \tau)$ which leads to $\langle x_0^2(\tau) \rangle$ as given by Eq. (7). Second, the dynamics of the decay is dependent on τ as shown explicitly in Eq. (8). Both effects move $\langle T \rangle$ in the same direction, i.e., increasing τ results in increasing $\langle T \rangle$.

Observing that $\ln x = \ln(10) \log_{10} x$, we can recast these results in the convenient form

$$\langle T \rangle = -m \log_{10} D + b(\tau) + B_0, \quad (9)$$

where

$$m = \frac{\ln 10}{2(A-1)}, \quad (10a)$$

and

$$B_0 = -m \log_{10} C \sim 0, \quad (10b)$$

so that $b(\tau)$ describes the combined dependence of $\langle T \rangle$ on the noise correlation time:

$$b(\tau) = -m \log_{10} \{ (|A_0| + 1)^{-1} [1 + \tau(|A_0| + 1)]^{-1} + (A-1)^{-1} [1 + \tau(A-1)]^{-1} \}. \quad (11)$$

These results can be accurate only in the range of small D . Indeed, we used linear theory to calculate $\langle x_0^2 \rangle$. Furthermore, Suzuki scaling is expected to be accurate only for small D , but here the quantitative limit is not known.

In the following sections we describe an analog simulation of Eqs. (1) and (2) for the range $0.1 \leq \tau \leq 5$ and for $10^{-6} \leq D \leq 10^{-1}$. Since $D = \tau \langle \xi^2 \rangle$, as shown by Eq. (2b), the range of D corresponds to a range of noise voltage $V_n \equiv \xi$ of somewhat less than three orders of magnitude, or about 10 mV to a few volts, which corresponds to the usable dynamic range of our analog simulators.

III. ANALOG SIMULATION

We have constructed a circuit model of Eqs. (1) and (2) using by now quite standard techniques.³² The schematic diagram of this simulator is shown on Fig. 2.

The noise voltage $V_n(t)$, is obtained from a Wandell

and Goltermann³³ wide band (> 100 kHz), Gaussian noise generator. In order to create colored noise, $V_n(t)$ is passed through a linear, single pole filter with a transfer function $H(\omega) = [1 + (\omega\tau_n)^2]^{-1}$, where ω is the radian frequency and τ_n the noise correlation time. The characteristic response time of the simulator is established by the integrator time constant τ_i , as shown on Fig. 2. The dimensionless noise correlation time, as it appears in the theory and in Eq. (2), is the ratio $\tau = \tau_n / \tau_i$. When $\tau \ll 1$, the simulator perceives the noise as quasiwhite, whereas $\tau \geq 1$ marks the colored-noise regime. With $V_n(t) \equiv \xi(t)$, Eq. (2b) defines the noise intensity $D = \tau \langle V_n^2 \rangle$ for $t = s$. The mean-square noise voltage $\langle V_n^2 \rangle$ is the measured quantity in our simulation which defines D . In this experiment we always maintained $D \leq 0.30$, and the correlation time varied over the range $0.1 \leq \tau \leq 5$.

In the absence of noise, the discrepancies between the deterministic steady states measured on the simulator are smaller than $\pm 2.5\%$ when compared to the steady-state ($\dot{x} = 0$) solutions of Eqs. (1) and (2a). Measurements in the presence of noise are, of course, subject to statistical errors which can be reduced by increasing the number of samples in a given average. In this experiment the statistical errors are estimated (from the repeatability) to be $\approx \pm 5\%$. The largest error, and the most difficult to quantify, is systematic and shows up in the quasiwhite noise end of the range of τ . This results from the limited dynamic range and bandwidth of the simulator. For τ small, $V_n(t)$ is large, and an increasing number of its large-amplitude excursions in the wings of the Gaussian are clipped as τ is decreased. At $\tau = 0.1$, this results in discrepancies between our measured probability densities and white-noise solutions of the FP equation which, in places, are as large as $\sim 20\%$. In this experiment, relaxation times are measured for which it is difficult to estimate the systematic errors at the small- τ end.

In operation, a rectangular wave $A(t)$, operating between the voltages A_0 and A was applied to the divider as shown in Fig. 2. The frequency of this wave was adjusted so that in the state A_0 sufficient time was allowed for the initial probability density of x to become stationary (several hundred times τ_i). The wave switches from A_0 to A at $t = 0$ and at the same time the data-analysis

TABLE II. Calculated and measured parameters for $A_0 = -1.38$, $A = 3$, and $B_0 = 0.07$.

τ	m^{theor}	m^{expt}	$b^{\text{theor}}(\tau)$	$b^{\text{theor}}(\tau) + B_0$	b^{expt}
4.9	0.58	0.58	0.63	0.70	0.70
1.0	0.58	0.58	0.31	0.38	0.39
0.5	0.58	0.58	0.20	0.27	0.31
0.1	0.58	0.57	0.07	0.14	0.28

TABLE III. Calculated and measured parameters for $A_0 = -2.4$, $A = 4.0$, and $B_0 = 0.16$.

τ	m^{theor}	m^{expt}	$b^{\text{theor}}(\tau)$	$b^{\text{theor}}(\tau) + B_0$	b^{expt}
5.0	0.38	0.39	0.55	0.71	0.71
1.0	0.38	0.39	0.32	0.48	0.47
0.5	0.38	0.39	0.24	0.40	0.39
0.1	0.38	0.38	0.12	0.28	0.35

system, a Nicolet-Lab 80 computer and digitizer connected to the circuit at $x(t)$, was triggered. A time series of typically 2000K digitized points was then obtained, and the time at which the trajectory first crossed the threshold $x_R = x_s/2$ ($x_s = \pm\sqrt{A-1}$ are the deterministic steady states) was measured and stored. Ten example trajectories are shown in Fig. 3, where the threshold is marked by arrows, and an example crossing time at T_i is shown. After a large number of such measurements (typically 10^4) the computer tabulates the mean-relaxation time $\langle T \rangle$ and its density $P(T)$. Three examples of the densities are shown in Fig. 4 for three values of D . As expected $\langle T \rangle$ increases as D becomes smaller.

IV. RESULTS

The results of our simulation are summarized on three graphs and compared to the theoretical predictions in three tables. Figure 5 shows our measured values of $\langle T \rangle$ versus D for four values of τ as indicated by the different symbols for $A_0 = -1.38$ and $A = 2.0$ V. Each set of data were matched by least-squares fit to the equation

$$\langle T \rangle = -m \log_{10} D + b, \quad (12)$$

and the values m^{expt} and b^{expt} were extracted. These were compared to the results predicted by Eqs. (9)–(11). As shown by Eq. (9) the entire colored-noise effect is represented by the constant $b(\tau)$. It is evident, however, that the non-color-dependent constant B_0 is not negligible. We obtained a value for B_0 by matching the experimental and theoretical results at $\tau = 4.9$ and 5 (where the simulation is most accurate) and then compared the predicted and observed values in Table I, where the $b^{\text{theor}}(\tau)$ and m^{theor} are calculated directly from Eqs. (10a) and (11), and b^{expt} is to be compared with $b^{\text{theor}}(\tau) + B_0$. The results are shown on Table I. The largest discrepancies are for $\tau = 0.5$ and 0.1 as expected. Even so, on the logarithmic scale of Fig. 5 the difference between Eq. (9) using the theoretical values and the data are small, as shown by the dashed line which is to be compared to the crosses $\tau = 0.5$. The solid lines through the data for $\tau = 0.1$ and $\tau = 4.9$ are example plots of the results of the least-squares fits of the data to Eq. (12).

Figure 6 and Table II show the results for $A_0 = -1.38$ and $A = 3.0$. It is evident that while B_0 has changed con-

siderably, the discrepancy at $\tau = 0.1$ is decreased. Figure 7 and Table III show the results for $A_0 = -2.4$ and $A = 4$. On Fig. 7 we also show the theoretical result for $\tau = 1.0$ as the dot-dashed line to be compared with the open circles. The dashed line is the prediction for $\tau = 0.1$ and shows the largest disagreement with the measurements (closed circles).

V. CONCLUSIONS AND DISCUSSION

The agreement between the calculated and the measured results in this work is satisfactory considering the approximations necessary to achieve a colored-noise theory. We emphasize further that the strictly colored-noise contributions to the theory have two sources: the decay theory of Dhara and Menon²³ and the *ansatz*.¹² The latter, which agrees with the linearization result in Eq. (7), can be used to calculate the second moment of the initial, stationary ($t < 0$) density, an application for which it is known to be relatively accurate. The relative importance of each of these contributions depends on A_0 and A as shown by the two terms in brackets in Eq. (11). For small A_0 and large A , $\langle x_0^2 \rangle$ dominates the decay process and hence the *ansatz* is more important, while for large A_0 and small A the reverse is true, and the non-linear decay process dominates. We conclude by pointing out that colored-noise-driven decay of unstable states should find applications in a variety of switching scenarios most notably in laser dynamics and nonlinear optical bistability.

ACKNOWLEDGEMENTS

Two of us (F.M. and P.H.) are grateful to the Physics Departments of the University of Lancaster, U. K. and Limburg's University Centrum, Belgium for their hospitality during which part of this work was carried out. We are pleased to acknowledge stimulating discussions with F. T. Arecchi, E. Arimondo, W. Ebeling, L. A. Lugiatto, P. Mandel, F. Marchesoni, L. Narducci, H. Risken, R. Roy, J. M. Sancho, M. San Miguel, and J. Tredicce. This work was supported in part by the British Science and Engineering Research Council, the Belgian National Foundation for Scientific Research, NATO Grant No. RG. 85/0770, and the U. S. Office of Naval Research Grant No. N00014-88-K-0084.

*Present address: Division of Science, University of Wisconsin at Parkside, Kenosha, WI 53141.

¹R. W. Keyes and R. Landauer, IBM J. Res. Dev. **14**, 152 (1970); R. Landauer, Appl. Phys. Lett. **51**, 2056 (1987); in *Der*

Informationsbegriff in Technik und Wissenschaft, edited by O. G. Folberth and C. Hackl (Oldenbourg, Munich, 1986), p. 139.

²R. Landauer, Phys. Scr. **35**, 88 (1987); C. H. Bennett, Sci. Am.

- 257, 108 (1987); C. H. Bennett and R. Landauer, *ibid.* **253**, 48 (1985). For a review see C. H. Bennett, *Int. J. Theor. Phys.* **21**, 905 (1982).
- ³D. K. Kondepudi, F. Moss, and P. V. E. McClintock, *Physica (Utrecht)* **21D**, 296 (1986).
- ⁴(a) S. Zhu, A. W. Yu, and R. Roy, *Phys. Rev. A* **34**, 4333 (1986); (b) G. Broggi, A. Colombo, L. A. Lugiato, and P. Mandel, *ibid.* **33**, 3635 (1986).
- ⁵R. Mannella, F. Moss, and P. V. E. McClintock, *Phys. Rev. A* **35**, 2560 (1987).
- ⁶For an authoritative review, see M. Suzuki, *Adv. Chem. Phys.* **46**, 195 (1981).
- ⁷P. de Pasquale and P. Tombesi, *Phys. Lett.* **72A**, 7 (1979).
- ⁸For a collection of recent reviews, see *Rate Processes and First Passage Times*, edited by G. H. Weiss [*J. Stat. Phys.* **42**, 1 (1986)].
- ⁹Matrix continued-fraction technique offer solutions of two-dimensional FP equations which are, in principle, exact. See H. Risken, *The Fokker-Planck Equation* (Springer-Verlag, Berlin 1984). The necessity to invert and hence truncate a final matrix of infinite dimension limits the practical application of the technique, using ordinary computers, to two-dimensional problems. For MCF theory applied to the decay of an unstable state, see P. Jung and H. Risken, *Z. Phys. B* **59**, 469 (1985).
- ¹⁰P. Hanggi and P. Talkner, *Phys. Rev. Lett.* **51**, 2242 (1983).
- ¹¹J. M. Sancho, M. San Miguel, S. Katz, and J. D. Gunton, *Phys. Rev. A* **26**, 1589 (1982).
- ¹²P. Hanggi, T. J. Mroczkowski, F. Moss, and P. V. E. McClintock, *Phys. Rev. A* **32**, 695 (1985).
- ¹³R. F. Fox, *Phys. Rev. A* **33**, 467 (1986); **34**, 4525 (1986).
- ¹⁴P. Jung and P. Hanggi, *Phys. Rev. A* **35**, 4464 (1987).
- ¹⁵M. Dygas, B. J. Matkowsky, and Z. Schuss, *SIAM J. Appl. Math.* **48**, 425 (1988).
- ¹⁶C. R. Doering, P. S. Hagan, and C. D. Levermore, *Phys. Rev. Lett.* **59**, 2129 (1987).
- ¹⁷R. F. Fox, *Phys. Rev. A* **37**, 911 (1988).
- ¹⁸See the various articles in *Noise in Nonlinear Dynamical Systems*, edited by F. Moss and P. V. E. McClintock (Cambridge University Press, Cambridge, 1989), Vol. I.
- ¹⁹P. Jung and P. Hänggi, *Phys. Rev. Lett.* **61**, 11 (1988).
- ²⁰R. L. Stratonovich, *Topics in the Theory of Random Noise* (Gordon and Breach, New York, 1963), Vol. I.
- ²¹For a review see, N. G. Van Kampen, *Phys. Rep.* **24C**, 171 (1976).
- ²²F. Moss, P. Hänggi, R. Mannella, and P. V. E. McClintock, *Phys. Rev. A* **33**, 4459 (1986).
- ²³A. K. Dhara and S. V. G. Menon, *J. Stat. Phys.* **46**, 743 (1987).
- ²⁴F. T. Arecchi, A. Politi, and L. Ulivi, *Nuovo Cimento* **71B**, 119 (1982).
- ²⁵G. Broggi, L. A. Lugiato, and A. Colombo, *Phys. Rev. A* **32**, 2803 (1985).
- ²⁶R. Kubo, K. Matsuo, and K. Kitahara, *J. Stat. Phys.* **9**, 51 (1971).
- ²⁷F. T. Arecchi, V. Degiorgio, and B. Querzola, *Phys. Rev. A* **3**, 1108 (1971); F. T. Arecchi and A. Politi, *Phys. Lett.* **45**, 1219 (1980).
- ²⁸F. Haake, *Phys. Rev. Lett.* **41**, 1685 (1978).
- ²⁹U. Weiss, *Phys. Rev. A* **25**, 2444 (1982).
- ³⁰F. de Pasquale, P. Tataglia, and P. Tombesi, *Phys. Rev. A* **25**, 466 (1982).
- ³¹M. Suzuki, *Prog. Theor. Phys.* **56**, 77 (1976); **56**, 477 (1976); **57**, 380 (1977).
- ³²For a review, see P. V. E. McClintock and F. Moss, in Ref. 18, Vol. III, Chap. 9.
- ³³Wendel and Goltermann, GmbH & Co., P. O. Box 45, D7412 Eningen, Federal Republic of Germany.